

The application of some nuclear potentials for quasielastic scattering data of the $^{11}\text{Li} + ^{28}\text{Si}$ reaction and its consequences

Murat AYGÜN*

Department of Physics, Faculty of Science, Bitlis Eren University, Bitlis, Turkey

Received: 06.01.2018

Accepted/Published Online: 09.04.2018

Final Version: 01.06.2018

Abstract: The aim of the present study is to provide a better understanding of the effect and applicability of nuclear potentials on scattering reactions. For this, we investigate the quasielastic scattering data of the $^{11}\text{Li} + ^{28}\text{Si}$ reaction at 319 MeV within the framework of the optical model. In order to obtain the real part of the optical potential, we use ten different potentials, which consist of Proximity 1977 (Prox 77), Proximity 1988 (Prox 88), Broglia and Winther 1991 (BW 91), Aage Winther (AW 95), Christensen and Winther 1976 (CW 76), Bass 1973 (Bass 73), Bass 1977 (Bass 77), Bass 1980 (Bass 80), Siwek-Wilczynska–Wilczynski (SWW), and Denisov potential (DP). The imaginary part is assumed as Woods–Saxon type in all the calculations. The theoretical results are compared with each other as well as the experimental data. It is found that the results depend on the shapes of the nuclear potentials used in the analysis. The most consistent results with the experimental data are obtained for Prox 77 potential. Finally, the cross-sections (σ) and χ^2/N values are given for all the nuclear potential calculations.

Key words: Proximity potential, nuclear potential, optical model

1. Introduction

The nuclear potential that describes the interaction of two nuclei is very necessary in providing accurate and meaningful explanations of nuclear reactions. Thus, more reliable information about the structure of a nucleus can be obtained by using suitable potential parameters. These potentials sometimes depend on the potential depths, sometimes their energies, or sometimes the nucleon number or charge of target nuclei. Although the Coulomb potential due to the charges of the nuclei is well described, the nuclear potential could not be exactly described. In this context, although different nuclear potentials can be obtained from the literature, this subject is still a problem of interest in the field of nuclear physics. For this reason, the introduction of alternative potentials will be very important in explaining different nuclear interactions such as elastic scattering, inelastic scattering, and coupled channels.

Halo nuclei are a hot topic in the field of nuclear physics because of their properties such as root mean square (rms) values, different density distributions, and low binding energies. In this sense, ^{11}Li , which is well known as a neutron halo nucleus, has a large number of both experimental and theoretical studies. One of the most interesting experimental topics is the $^{11}\text{Li} + ^{28}\text{Si}$ reaction. In order to explain this reaction, a considerable number of studies have been carried out using different approaches and models so far. Lewitowicz et al. [1] measured the quasielastic scattering data of ^{11}Li on the ^{28}Si target at 319 MeV. They performed the theoretical

*Correspondence: maygun@beu.edu.tr

analysis by using both phenomenological potential and double folding potential. Al-Khalili [2] examined the projectile breakup channel effect on $^{11}\text{Li} + ^{28}\text{Si}$ elastic scattering at 29 MeV/nucleon by using the four-body Glauber scattering model. Cooper and Mackintosh [3] achieved agreement results with the data by applying two-step phenomenology. Fayans et al. [4] carried out coupled-channels calculations in the double folding approach for the quasielastic scattering data of the $^{11}\text{Li} + ^{28}\text{Si}$ reaction. Carstoiu and Lassaut [5] performed an optical model analysis of ^6Li and ^{11}Li scattered from ^{12}C and ^{28}Si target nuclei. While a good fit with the experimental data was acquired for $^{11}\text{Li} + ^{12}\text{C}$ reaction, a similar result could not be obtained for the $^{11}\text{Li} + ^{28}\text{Si}$ reaction. Rashdan [6] investigated the elastic scattering of ^{11}Li by ^{12}C and ^{28}Si within the framework of the relativistic mean field theory. Pacheco and Mau [7] analyzed the quasielastic scattering of the $^{11}\text{Li} + ^{28}\text{Si}$ system and found unsatisfactory results with the experimental data. Un et al. [8] studied the quasielastic scattering of the $^{11}\text{Li} + ^{28}\text{Si}$ reaction at 29 MeV/nucleon within the framework of the coupled-channels model and acquired good agreement with the data. Canbula et al. [9] examined by using the coupled-channels method the quasielastic scattering data of ^{11}Li by the ^{28}Si target nucleus at 319 MeV. The experimental data are still not very well understood although the theoretical results describing the data have been improved with these studies.

In the present work, we aim to examine the role of nuclear potential in explaining the experimental data of the $^{11}\text{Li} + ^{28}\text{Si}$ reaction under the optical model. In order to obtain the real part of the optical potential, we use ten different nuclear potentials, which include Proximity 1977 (Prox 77) [10], Proximity 1988 (Prox 88) [10], Broglia and Winther 1991 (BW 91) [11], Aage Winther (AW 95) [12], Christensen and Winther 1976 (CW 76) [13], Bass 1973 (Bass 73) [14,15], Bass 1977 (Bass 77) [16], Bass 1980 (Bass 80) [11], Siwek-Wilczynska-Wilczynski (SWW) [17,18], and Denisov potential (DP) [19,20]. We assume Woods-Saxon (WS) potential for the imaginary part in all the theoretical calculations. Then we compare the theoretical results with both each other and the literature as well as the experimental data. Finally, we give the cross-sections (σ) and χ^2/N values of all the nuclear potential calculations investigated in this study.

The next section provides information on the method and nuclear potentials used in our work. Section 3 shows the results and discussion. Finally, Section 4 is assigned to the conclusion.

2. Theoretical formalism

2.1. Optical model

The optical model is one of the simplest and the most successful models in calculating the elastic scattering cross-sections of nuclear reactions. The potential defined by means of the optical model is assumed as the optical potential. The optical potential consists of the real potential and the imaginary potential. While the real part is responsible for elastic scattering, the imaginary part shows absorption. The optical potential is also nonlocal, energy-dependent, and complex. To obtain the real part of the optical potential in our study, ten different potentials have been evaluated. Each of these potentials has been described in the following section. The imaginary part has been taken as the WS potential, which is given by

$$W(r) = \frac{W_0}{\left[1 + \exp\left(\frac{r-R_w}{a_w}\right)\right]}, \quad (1)$$

where W_0 , R_w , and a_w are depth, radius, and diffuseness parameters of the imaginary part, respectively.

Thus, the total interaction potential between projectile and target nuclei can be written as

$$V_{total}(r) = V_C(r) + V_N(r), \quad (2)$$

where V_C is Coulomb potential and V_N is nuclear potential. $V_C(r)$ potential is shown by [21]

$$V_C(r) = \frac{1}{4\pi\epsilon_0} \frac{Z_P Z_T e^2}{r} \quad r \geq R_C, \quad (3)$$

$$= \frac{1}{4\pi\epsilon_0} \frac{Z_P Z_T e^2}{2R_C} \left(3 - \frac{r^2}{R_C^2} \right), \quad r \leq R_C, \quad (4)$$

where R_c is the Coulomb radius, taken as $1.25(A_P^{1/3} + A_T^{1/3})$ fm in the calculations. The code FRESKO has been applied in the optical model calculations [22].

2.2. Nuclear potentials

In the present work, in order to see the effects of different nuclear potentials in defining the quasielastic scattering data of the $^{11}\text{Li} + ^{28}\text{Si}$ reaction, we evaluate ten different nuclear potentials: Proximity 1977 (Prox 77), Proximity 1988 (Prox 88), Broglia and Winther 1991 (BW 91), Aage Winther (AW 95), Christensen and Winther 1976 (CW 76), Bass 1973 (Bass 73), Bass 1977 (Bass 77), Bass 1980 (Bass 80), Siwek-Wilczynska-Wilczynski (SWW), and Denisov potential (DP). Information about the potentials is given in the following subsections.

2.2.1. Proximity 1977 (Prox 77) potential

According to Prox 77 potential, $V_N(r)$ potential [10] is

$$V_N^{\text{Pr ox 77}}(r) = 4\pi\gamma b \bar{R} \Phi \left(\zeta = \frac{r - C_1 - C_2}{b} \right) \text{ MeV}, \quad (5)$$

where

$$\bar{R} = \frac{C_1 C_2}{C_1 + C_2}, \quad C_i = R_i \left[1 - \left(\frac{b}{R_i} \right)^2 + \dots \right]. \quad (6)$$

R_i , the effective radius, is

$$R_i = 1.28 A_i^{1/3} - 0.76 + 0.8 A_i^{-1/3} \text{ fm} \quad (i = 1, 2). \quad (7)$$

γ , the surface energy coefficient, is,

$$\gamma = \gamma_0 \left[1 - k_s \left(\frac{N - Z}{N + Z} \right)^2 \right], \quad (8)$$

where N and Z are the total numbers of neutrons and protons, respectively. Also, the value of γ_0 is 0.9517 MeV/fm² and k_s is 1.7826. The universal function ($\Phi(\zeta)$) can be written as follows.

$$\Phi(\zeta) = \begin{cases} -\frac{1}{2} (\zeta - 2.54)^2 - 0.0852 (\zeta - 2.54)^3, & \text{for } \zeta \leq 1.2511 \\ -3.437 \exp\left(-\frac{\zeta}{0.75}\right), & \text{for } \zeta \geq 1.2511 \end{cases} \quad (9)$$

2.2.2. Proximity 1988 (Prox 88) potential

Möller and Nix [23] advanced the mass formula with new values of γ_0 and k_s given in Eq. (8). These values are 1.2496 MeV/fm² for γ_0 and 2.3 for k_s [11], which display a stronger attraction. The other parameters of Prox 88 potential are the same as Prox 77 potential.

2.2.3. Broglia and Winther 1991 (BW 91) potential

In this approach, the real part of the optical potential is assumed as [19]

$$V_N^{BW91}(r) = -\frac{V_0}{[1 + \exp(\frac{r-R_0}{a})]} \text{ MeV}, \quad (10)$$

where

$$V_0 = 16\pi \frac{R_1 R_2}{R_1 + R_2} \gamma a, \quad a = 0.63 \text{ fm}, \quad (11)$$

and

$$R_0 = R_1 + R_2 + 0.29, \quad R_i = 1.233A_i^{1/3} - 0.98A_i^{-1/3} \text{ fm} \quad (i = 1, 2). \quad (12)$$

The surface energy constant γ is

$$\gamma = \gamma_0 \left[1 - k_s \left(\frac{N_P - Z_P}{A_P} \right) \left(\frac{N_T - Z_T}{A_T} \right) \right]. \quad (13)$$

γ_0 and k_s are taken as 0.95 MeV/fm² and 1.8, respectively.

2.2.4. Aage Winther (AW 95) potential

The fourth kind of potential employed for the real part is the same as BW 91 potential except for [19]

$$a = \left[\frac{1}{1.17 \left(1 + 0.53 \left(A_1^{-1/3} + A_2^{-1/3} \right) \right)} \right] \text{ fm}, \quad (14)$$

and

$$R_0 = R_1 + R_2, \quad R_i = 1.2A_i^{1/3} - 0.09 \quad (i = 1, 2). \quad (15)$$

2.2.5. Christensen and Winther 1976 (CW 76) potential

Another form of the real potential analyzed with this work is written as [24]

$$V_N^{CW76}(r) = -50 \frac{R_1 R_2}{R_1 + R_2} \phi(r - R_1 - R_2) \text{ MeV}, \quad (16)$$

where

$$R_i = 1.233A_i^{1/3} - 0.978A_i^{-1/3} \text{ fm} \quad (i = 1, 2). \quad (17)$$

The universal function $\phi(s = r - R_1 - R_2)$ is

$$\phi(s) = \exp\left(-\frac{r - R_1 - R_2}{0.63}\right). \quad (18)$$

2.2.6. Bass 1973 (Bass 73) potential

The sixth potential for the real part is parameterized as [24]

$$V_N^{Bass73}(r) = -\frac{da_s A_1^{1/3} A_2^{1/3}}{R_{12}} \exp\left(-\frac{r - R_{12}}{d}\right) \text{ MeV}, \quad (19)$$

where

$$R_{12} = 1.07 \left(A_1^{1/3} + A_2^{1/3} \right), \quad d = 1.35 \text{ fm}, \quad a_s = 17 \text{ MeV}. \quad (20)$$

2.2.7. Bass 1977 (Bass 77) potential

Another real potential is in the following form [19]:

$$V_N^{Bass77}(s) = -\frac{R_1 R_2}{R_1 + R_2} \phi(s = r - R_1 - R_2) \text{ MeV}, \quad (21)$$

where

$$R_i = 1.16 A_i^{1/3} - 1.39 A_i^{-1/3} \text{ fm} \quad (i = 1, 2). \quad (22)$$

The universal function $\phi(s = r - R_1 - R_2)$ is assumed as

$$\phi(s) = \left[A \exp\left(\frac{s}{d_1}\right) + B \exp\left(\frac{s}{d_2}\right) \right]^{-1}, \quad (23)$$

where

$$A = 0.030 \text{ MeV}^{-1} \text{ fm}, \quad B = 0.0061 \text{ MeV}^{-1} \text{ fm}, \quad d_1(d_2) = 3.30(0.65) \text{ fm}. \quad (24)$$

2.2.8. Bass 1980 (Bass 80) potential

This potential is the same as Bass 77 potential. Only the function $\phi(s = r - R_1 - R_2)$ is different and is given by [19]

$$\phi(s) = \left[0.033 \exp\left(\frac{s}{3.5}\right) + 0.007 \exp\left(\frac{s}{0.65}\right) \right]^{-1}, \quad (25)$$

and

$$R_i = R_s \left(1 - \frac{0.98}{R_s^2} \right), \quad R_i = 1.28 A_i^{1/3} - 0.76 + 0.8 A_i^{-1/3} \text{ fm} \quad (i = 1, 2). \quad (26)$$

2.2.9. Siwek-Wilczynska-Wilczynski (SWW) potential

SWW potential, which is based on the liquid drop model and with the WS potential, is given as [17,18]

$$V_N^{SWW}(r) = -\frac{V_0}{\left[1 + \exp\left(\frac{r - R_1 - R_2}{a}\right) \right]} \text{ MeV}, \quad (27)$$

where

$$V_0 = b_{surf} \left[A_1^{2/3} + A_2^{2/3} - (A_1 + A_2)^{2/3} \right], \quad b_{surf} \approx 17 \text{ MeV}, \quad (28)$$

and

$$R_i = 1.128A_i^{1/3} \left(1 - 0.786A_i^{-2/3}\right) \quad (i = 1, 2), \quad (29)$$

with

$$a = \frac{V_0(R_1 + R_2)}{16\pi\gamma R_1 R_2}, \quad \gamma = 0.9517 \left[1 - 1.7826 \left(\frac{N_P + N_T - Z_P - Z_T}{A_P + A_T}\right)\right] \text{ MeV fm}^{-2}. \quad (30)$$

2.2.10. Denisov potential (DP)

DP is last potential type used in the analysis of nuclear interactions. It is given by [19,20]

$$\begin{aligned} V_N^{DP}(r) = & -1.989843 \frac{R_1 R_2}{R_1 + R_2} \phi(r - R_1 - R_2 - 2.65) \\ & \times \left[1 + 0.003525139 \left(\frac{A_1}{A_2} + \frac{A_2}{A_1}\right)^{3/2} - 0.4113263 (I_1 + I_2)\right] \text{ MeV}, \end{aligned} \quad (31)$$

where

$$I_i = \frac{N_i - Z_i}{A_i}, \quad (32)$$

and

$$R_i = R_{ip} \left(1 - \frac{3.413817}{R_{ip}^2}\right) + 1.284589 \left(I_i - \frac{0.4A_i}{A_i + 200}\right), \quad (33)$$

$$R_{ip} = 1.24A_i^{1/3} \left(1 + \frac{1.646}{A_i} - 0.191 \left(\frac{A_i - 2Z_i}{A_i}\right)\right) \text{ fm} \quad (i = 1, 2). \quad (34)$$

The universal function $\phi(s = r - R_1 - R_2 - 2.65)$ is assumed as

$$\phi(s) = \begin{cases} 1 - \frac{s}{0.7881663} + 1.229218s^2 - 0.2234277s^3 - 0.1038769s^4 - \\ \frac{R_1 R_2}{R_1 + R_2} (0.1844935s^2 + 0.07570101s^3 + \\ (I_1 + I_2) (0.04470645s^2 + 0.0334687s^3) & (-5.65 \leq s \leq 0), \\ \left(1 - s^2 \left(\frac{0.05410106}{R_1 + R_2} \frac{R_1 R_2}{R_1 + R_2} \exp\left(-\frac{s}{1.76058}\right) - \right)\right) \exp\left(-\frac{s}{0.7881663}\right) & (s \geq 0). \end{cases} \quad (35)$$

3. Results and discussion

The elastic scattering angular distributions of the $^{11}\text{Li} + ^{28}\text{Si}$ system at 319 MeV have been obtained by using ten different nuclear potentials within the framework of the optical model. The distance-dependent variations of the potentials used in acquiring the real part of the optical potential are shown in Figure 1. The W_0 , r_w , and a_w parameters of the imaginary part assumed as the WS potential have been investigated to obtain results consistent with the experimental data. In this context, the r_w value has been examined in the range of 0.9–1.4 fm. The a_w value has been evaluated from 0.3 to 1.0 fm. The analysis has been completed by investigating the W_0 value. All the potential parameters are listed in the Table. The σ values are given for all the potential

calculations in the Table. We have observed that the σ values are between 1376 mb and 1966 mb except for DP (626 mb). We think that the reason for the small cross-section of the DP potential cannot explain the forward angles of the experimental data.

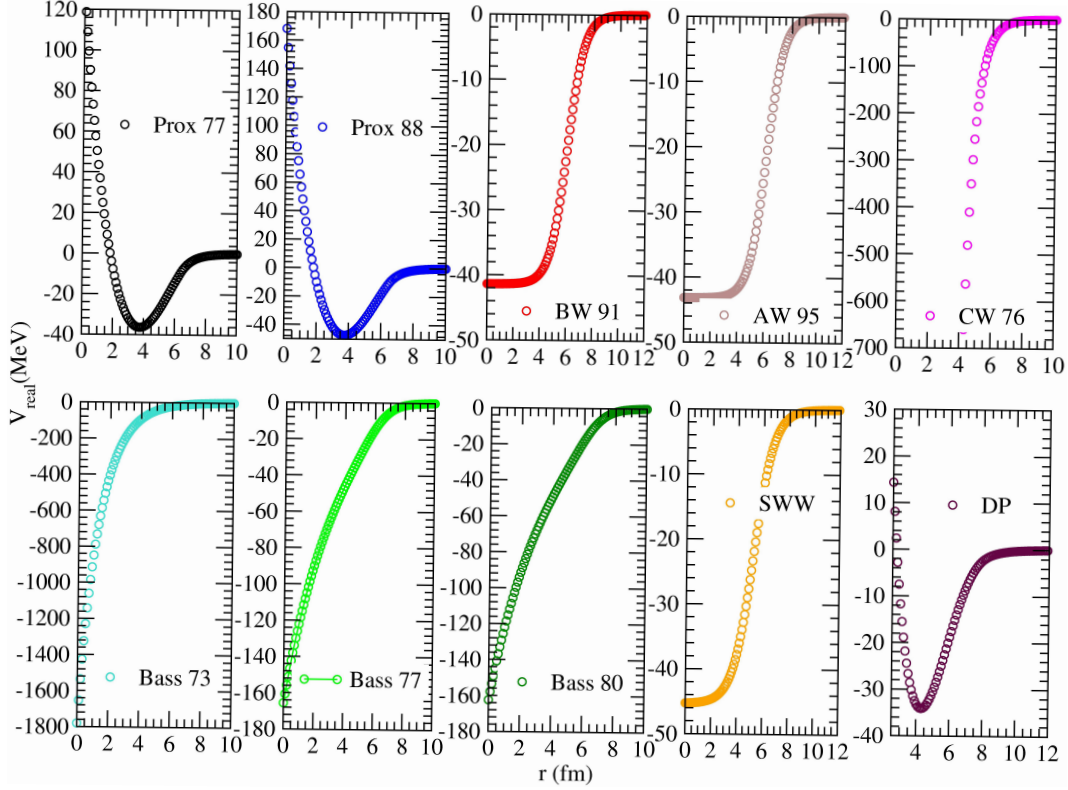


Figure 1. Distance-dependent changes of Prox 77, Prox 88, BW 91, AW 95, CW 76, Bass 73, Bass 77, Bass 80, SWW, and DP potentials.

Table. The imaginary potential parameters (W_0 , r_w , a_w), the cross-section (σ), and χ^2/N values obtained from the analysis with Prox 77, Prox 88, AW 95, BW 91, CW 76, Bass 73, Bass 77, Bass 80, SWW, and DP potentials of the $^{11}\text{Li} + ^{28}\text{Si}$ reaction at 319 MeV.

Potential type	W_0 (MeV)	r_w (fm)	a_w (fm)	σ (mb)	χ^2/N
Prox 77	26.3	0.940	0.70	1376.8	14.70
Prox 88	37.0	0.955	0.70	1530.5	26.51
AW 95	8.00	1.390	0.70	1966.1	23.41
BW 91	5.70	1.395	0.55	1669.1	60.37
CW 76	7.60	1.375	0.30	1557.4	189.8
Bass 73	15.3	1.230	0.30	1479.6	18.14
Bass 77	7.45	1.395	0.30	1628.1	33.90
Bass 80	7.70	1.387	0.31	1638.5	35.27
SWW	5.00	1.395	0.30	1454.7	19.87
DP	3.80	0.950	0.70	626.0	52.88

We compare our results with the experimental data in Figure 2. We have observed that Prox 77, Prox 88, AW 95, Bass 73, Bass 77, and Bass 80 potentials have given good results through the experimental data.

BW 91 results are missing the middle part of the experimental data. While CW 76, SWW, and DP results are not in good agreement with the data at forward angles, the results are good backwards angles.

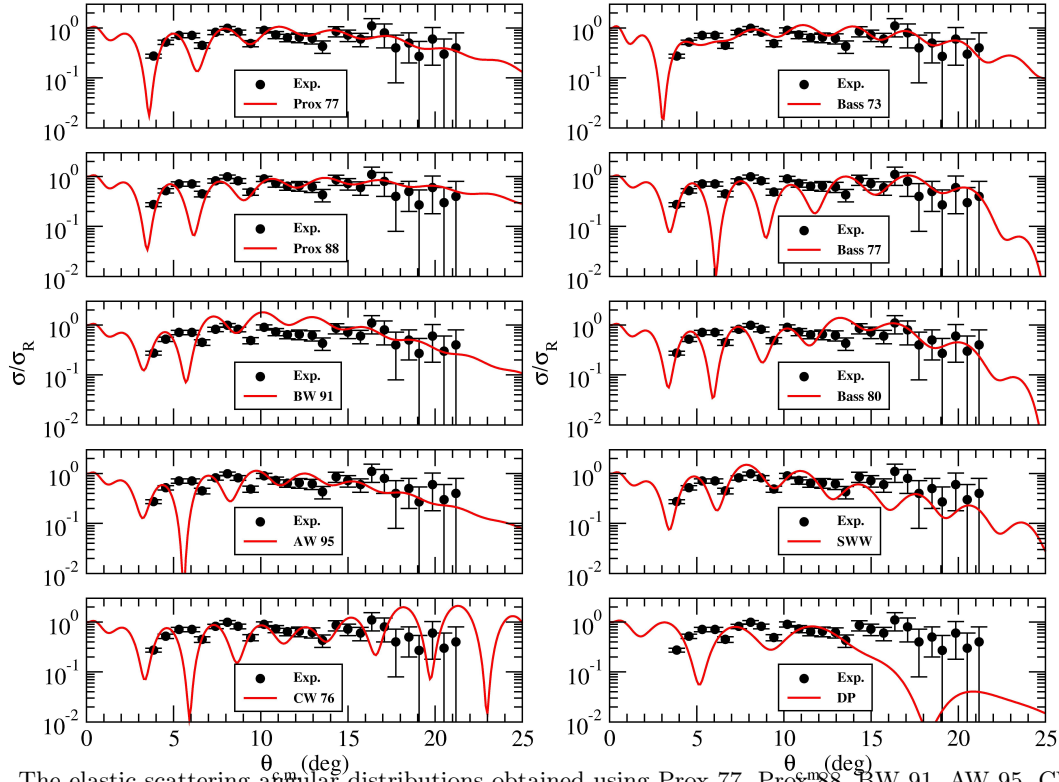


Figure 2. The elastic scattering angular distributions obtained using Prox 77, Prox⁸⁸, BW 91, AW 95, CW 76, Bass 73, Bass 77, Bass 80, SWW, and DP potentials of the $^{11}\text{Li} + ^{28}\text{Si}$ reaction at 319 MeV. The experimental data are taken from Ref. [1].

In Figure 3, we compare all the results with each other as well as the experimental data. We have observed that the results change according to the shape of the potential. In this context, the results of Prox 77 potential are better than the results of the other potentials. This situation has also been seen from the χ^2/N results. The results of Bass 73 potential are close to the results of Prox 77 potential in terms of both the χ^2/N value and the experimental data. However, there is a difference between the amplitudes.

When examining the results of Prox 88, AW 95, Bass 77, and Bass 80 potentials, it has been seen that the behaviors of the potential results are similar to each other at backward angles and the phase difference between them is more distinct. The differences between the amplitudes become clear at forward angles. The results of Prox 88 potential are more compatible with experimental data than the results of AW 95, Bass 77, and Bass 80 potentials.

The BW 91, CW 76, SWW, and DP potential results are not in good agreement with the experimental data. It has been observed that DP potential is far from defining the experimental data at forward angles. The amplitude of CW 76 potential is also very large compared to the experimental data, especially at forward angles. The greatest χ^2/N values are available for the BW 91, CW 76, and DP potentials.

In Figure 4, we compare our best results (Prox 77 and Bass 73) with the literature [9]. We have observed that the results of Prox 77 potential are better than the results of Ref. [9] and Bass 73 potential. The behaviors

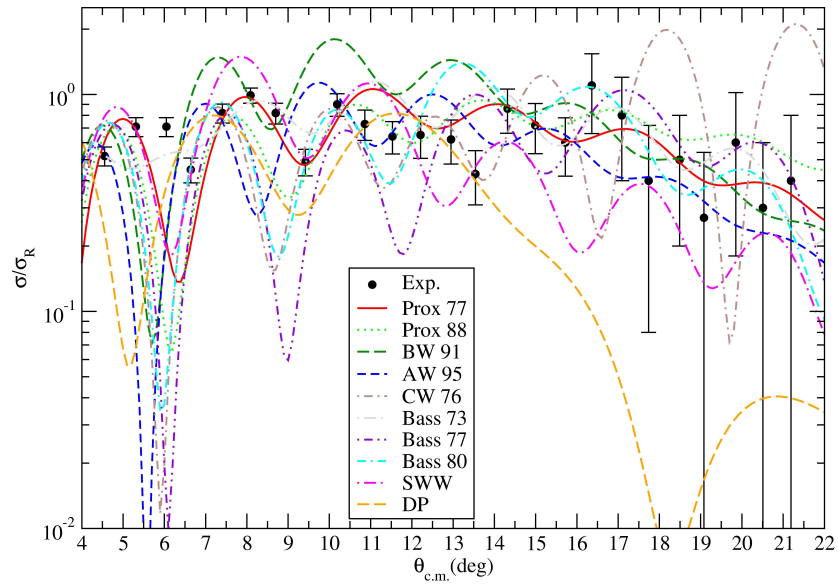


Figure 3. Comparison with both the experimental data and each other for elastic scattering angular distributions for Prox 77, Prox 88, BW 91, AW 95, CW 76, Bass 73, Bass 77, Bass 80, SWW, and DP potentials. The experimental data are taken from Ref. [1].

of Ref. [9] and Bass 73 potential are similar at forward angles. This similarity increases between $12^\circ < \Theta < 18^\circ$, but there is an amplitude difference between them. In addition, the phase difference becomes more distinct at further angles.

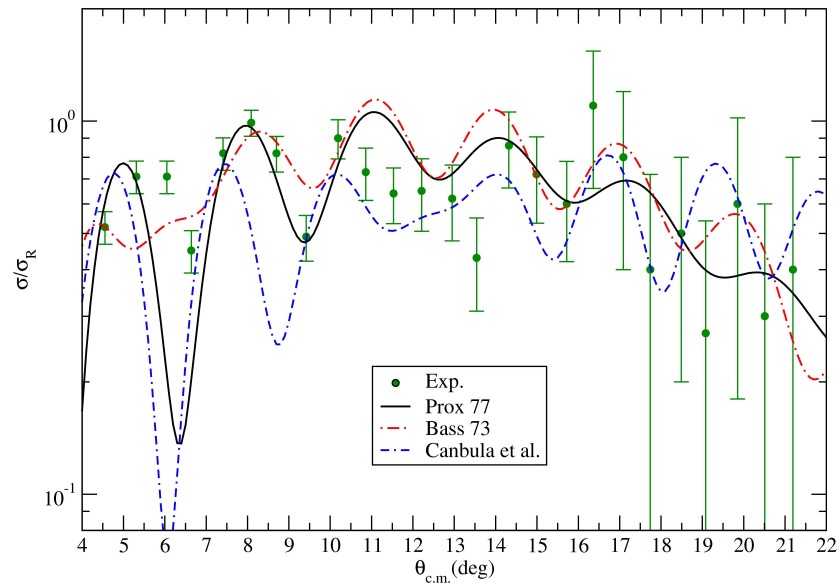


Figure 4. Comparison of the results of Prox 77, Bass 73, and the literature [9]. The experimental data are taken from Ref. [1].

4. Conclusion

In the present study, we have examined the effects of different nuclear potentials on the scattering data of the $^{11}\text{Li} + ^{28}\text{Si}$ system at 319 MeV. We have obtained the elastic scattering cross-sections by using ten various nuclear potentials within the optical model. We have observed that the theoretical results depend on the shape of the nuclear potential used in the analysis. In this context, the most consistent results with the experimental data have been obtained with Prox 77 potential, while the worst results have been found for DP potential. We consider that these potentials would be useful and interesting in applying to scattering data of different nucleus–nucleus interactions.

Acknowledgments

The author would like to thank the referees for valuable comments. The author would also like to thank Bora Canbula for providing his results in order to make a comparative study.

References

- [1] Lewitowicz, M.; Borcea, C.; Carstoiu, F.; Saint-Laurent, M. G.; Kordyas, A.; Anne, R.; Roussel-Chomaz, P.; Bimbot, R.; Borrel, V.; Dogny, S. et al. *Nucl. Phys. A* **1993**, *562*, 301-316.
- [2] Al-Khalili, J. *Nucl. Phys. A* **1995**, *581*, 315-330.
- [3] Cooper, S.; Mackintosh, R. *Nucl. Phys. A* **1995**, *582*, 283-295.
- [4] Fayans, S.; Knyazkov, O.; Kuchina, I.; Penionzhkevich, Y. E.; Skobelev, N. *Phys. Lett. B* **1995**, *357*, 509-514.
- [5] Carstoiu, F.; Lassaut, M. *Nucl. Phys. A* **1996**, *597*, 269-297.
- [6] Rashdan, M. *Phys. Rev. C* **1996**, *54*, 315-318.
- [7] Pacheco, J.; Vinh Mau, N. *Nucl. Phys. A* **2000**, *669*, 135-149.
- [8] Un, A.; Kucuk, Y.; Caner, T.; Boztosun, I. *Phys. Rev. C* **2014**, *89*, 057605.
- [9] Canbula, B.; Canbula, D.; Babacan, H. *Phys. Rev. C* **2015**, *91*, 044615.
- [10] Błocki, J.; Randrup, J.; Świątecki, W. J.; Tsang, C. F. *Ann. Phys. (NY)* **1977**, *105*, 427-462.
- [11] Reisdorf, W. *J. Phys. G Nucl. Part. Phys.* **1994**, *20*, 1297-1353.
- [12] Winther, A. *Nucl. Phys. A* **1995**, *594*, 203-245.
- [13] Christensen, P. R.; Winther, A. *Phys. Lett. B* **1976**, *65*, 19-22.
- [14] Bass, R. *Nucl. Phys. A* **1974**, *231*, 45-63.
- [15] Bass, R. *Phys. Lett. B* **1973**, *47*, 139-142.
- [16] Bass, R. *Phys. Rev. Lett.* **1977**, *39*, 265-268.
- [17] Wilczyński, J.; Siwek-Wilczynska, K. *Phys. Lett. B* **1975**, *55*, 270-272.
- [18] Sen, N. V.; Darves-Blanc, R.; Gondrand, J. C.; Merchez, F. *Phys. Rev. C* **1979**, *20*, 969-976.
- [19] Zhang, G. L.; Yao, Y. J.; Guo, M. F.; Pan, M.; Zhang, G. X.; Liu, X. X. *Nucl. Phys. A* **2016**, *951*, 86-96.
- [20] Denisov, V. Yu. *Phys. Lett. B* **2002**, *526*, 315-321.
- [21] Satchler, G. R. *Direct Nuclear Reactions*; Oxford University Press: Oxford, UK, 1983.
- [22] Thompson, I. J. *Computer Phys. Rep.* **1988**, *7*, 167-212.
- [23] Möller, P.; Nix, J. R. *Nucl. Phys. A* **1981**, *361*, 117-146.
- [24] Dutt, I.; Puri, R. K. *Phys. Rev. C* **2010**, *81*, 064609.